INTERFACIAL ENTROPY OF TERT-BUTYL ALCOHOL

Issarly Rivas, Aly J. Castellanos-Suárez, Máximo García-Sucre and German Urbina-Villalba

SUMMARY

In a previous paper the interfacial entropy of tert-butyl-alcohol (TBA) at a heptane/water interface was evaluated using a du Noüy ring (Vásquez et al., 2002). Here, this problem is revisited using a more accurate instrument for interfacial measurements: the spinning drop tensiometer. The results differ considerably from the previous evaluations. A broad continuous distribution of interfacial entropy with a large maximum at a molar fraction of TBA (x_{TBA})= 0.01 is found. The height of the maximum and the concentration of TBA at which it occurs are similar to the ones exhibited by aqueous solutions of alcohol.

ENTROPÍA INTERFACIAL DEL ALCOHOL TERBUTÍLICO

Issarly Rivas, Aly J. Castellanos-Suárez, Máximo García-Sucre y German Urbina-Villalba

RESUMEN

En un trabajo previo, la entropía interfacial del alcohol terbutílico (TBA) en la interfase heptano/agua fue evaluada utilizando un anillo du Nöuy (Vásquez et al., 2002). En el presente trabajo, el problema es revisado utilizando un instrumento más adecuado para realizar medidas interfaciales: el tensiometro de gota giratoria. Los resultados difieren considerablemente de las evaluaciones previas. Se encontró una distibución continua de entropía interfacial con un máximo grande a una fracción molar de TBA (x_{TBA})= 0,01. La altura del máximo y la concentración de TBA a la cual es observado, son similares a los exhibidos por soluciones acuosas del alcohol.

Introduction

Still today a systematic study on the surface entropy of pseudo-ternary systems composed of oil, water and surfactant is not available. This is partially due to the high sensitivity of these measurements with respect to the composition of the system and its temperature (Johansson, 1974). However, theoretical calculations suggest that the critical points of interfacial entropy might indicate interfacial compositions at which the effective interaction between surfactant molecules is either favorable or unfavorable (Urbina-Villalba et al., 1997).

Glinski et al. (1998) demonstrated that the surface entropy of aqueous solutions of some co-surfactants show critical points when plotted as a function of the solute concentration (Chavepeyer et al., 1995; Glinski et al., 1995, 1998, 1996, 1999). Ethanol, n-butanol and tert-butanol show one maximum of interfacial entropy (Glinski et al., 1995, 1998), whereas propanol shows two maxima (Glinski et al., 1996) and methanol none (Glinski et al., 1998). Recently, Romero et al. (2009) published new data on the temperature dependence of the surface tension of aqueous solutions of pentanol and hexanol at several alcohol concentrations. It appears from this information that unlike small alkanols, alcohols with 'long' hydrophobic chains ($5 \leq N_C \leq 8$, where N_C is the number of carbon atoms in the alcohol molecule) do not show pronounced maxima of surface entropy, while still longer molecules ($N_C \geq 10$) are insoluble in water (Glinski et al., 1993).

Graciaa et al. (1993) showed that in a system composed of octane, water and poly-ethoxylated alkylphenols, small chain alcohols adsorb pronouncedly to the interface, acting as spacers between the surfactant molecules. As the molecular weight of the alcohol increases, its interfacial concentration decreases and its solubility in the oil phase increases. As a result, these molecules act as lipophilic linkers between the surfactant and the oil molecules, increasing the solubility of the amphiphile in the non-polar phase (Graciaa et al., 1993).

It is also known that the attainment of three phases in mixtures of oil, water and an ionic surfactant produces low and ultralow values of the interfacial tension between the immiscible phases (Salager et al., 1979; Bourrel et al., 1980). This property is commonly used to manufacture nanoemulsions (Maestro et al., 2008) and it is also employed to improve the efficiency of oil recovery from a reservoir (Healy et al., 1975). In order to produce three phases starting from oil and water, the affinity of the surfactant for these liquids must be balanced. In the case of ionic surfactants, the increase of the salt concentration lowers the solubility of the surfactant in the aqueous phase, favoring its transfer to the oil phase. In general, anionic surfactants with two hydrophobic branches like

Issarly Rivas. B.Sc. in Chemistry, Universidad Central de Venezuela (UCV). Professional Research Associate, Instituto Venezolano de Investigaciones Científicas (IVIC), Venezuela. e-mail: irivas@ivic.gob.ve.

Aly J. Castellanos-Suárez. Doctor of Science in Chemistry, UCV, Venezuela. Researcher, IVIC, Venezuela. e-mail: acastell@ivic.gob.ve

Máximo García-Sucre. Docteur d´Etat in Physics, Université de Paris, France. Researcher, IVIC, Venezuela. e-mail: mgs@ivic.gob.ve

German Urbina-Villalba. Doctor of Science in Chemistry, UCV, Venezuela. Researcher, IVIC, Venezuela. Address: Physical Chemistry of Colloids Laboratory, Center of Interdisciplinary Studies in Physics. IVIC. Apartado 20632, Caracas 1020A, Venezuela. e-mail: guv@ivic.gob.ve

ENTROPIA INTERFACIAL DO ÁLCOOL TERBUTÍLICO

Issarly Rivas, Aly J. Castellanos-Suárez, Máximo García-Sucre e German Urbina-Villalba

RESUMO

Em um trabalho anterior, a entropia interfacial do álcool terbutílico (TBA) na interfase heptano/agua foi avaliada utilizando um anel du Nöuy (Vásquez et al., 2002). No presente trabalho, o problema é revisado utilizando um instrumento mais adequado para realizar medidas interfaciais: o tensiômetro de gota giratória. Os resultados diferem consideravelmente das avaliações anteriores. Encontrou-se uma distribuição contínua de entropia interfacial com um máximo grande a uma fração molar de TBA(x_{TBA})= 0.01. A altura do máximo e a concentração de TBA à qual é observado são similares aos exibidos por soluções aquosas do álcool.

2-bis-ethyl-hexyl sulfosuccinate (AOT) produce three phases and ultralow interfacial tensions in the presence of a suitable amount of sodium chloride (Aveyard et al., 1988). However, in the vast majority of the cases, three phases do not occur unless an appropriate alcohol is added to the mixture (Salager et al., 1979). High-molecular-weight alcohols favor the transfer of the surfactant to the oil phase, while small alcohols increase its solubility in the water phase (Bourrel et al., 1980). This change of behavior occurs at $N_C = 4$.

Curiously, the most pronounced maximum of surface entropy found in aqueous solutions, corresponds to tert-butyl alcohol ($\sim 0.18 \times 10^{-3} J \cdot m^{-2} \cdot K^{-1}$, x_{TBA}= 0.01; Glinski et al., 1995; Vásquez et al., 2002). Since TBA forms clathrates in bulk water at x_{TBA}= 0.05 (Iwasaki and Fujiyama, 1977, 1979), the referred maximum was formerly ascribed to the presence of these structures at the interface. However, that assignment occurred previously to the finding of several maxima in other systems (Glinski et al., 1996). This led to complementary hypothesis which included phase transitions, structure-changing effects, aggregate formation, etc (Glinski et al., 1993, 1995, 1996, 1998, 1999; Chavepeyer et al., 1995; Vásquez et al., 2002).

In order to identify the origin of the surface behavior of TBA, our group carried out measurements of surface tension and interfacial tension in mixtures of: water+TBA, heptane+TBA, and water+heptane+TBA (Vásquez et al., 2002). For these studies, an instrument similar to the one employed by Glinski et al. (Chavepeyer et al., 1995; Glinski et al., 1995, 1996, 1998) in previous reports was used (K10-ST from Krüss). Unfortunately, the results were inconclusive. The systems with heptane showed several small maxima of considerable lower magnitude than the one of the TBA-water system. In the case of heptane+TBA, the highest maximum did not reach 1/5 of the one exhibited by the aqueous solutions of TBA. In the case of the ternary system, the critical points ranged from 1/10 to 1/3 of its height (Vásquez et al., 2002).

It is well known that the techniques of du Nöuy ring and Wilhelmy plate are very reliable for the measurement of the surface tension, but less appropriate for the evaluation of the interfacial tension. The ring method requires volume corrections which depend on its geometry and the density of the phases. The plate determination depends on the wettability of the liquids and requires a special procedure to correct the flotation of the probe in the lighter liquid. Hence, it was decided to confirm the previous findings using a more accurate instrument for interfacial measurements: using the spinning drop tensiometer.

Experimental Procedure

Chemicals

n-Heptane (H) (Mallinckrodt, 99.6% pure) was eluded twice through an aluminum oxide column of 3mm mesh (Sigma-Aldrich) prior to use. Water (W) was distilled and then purified using a Simplicity system (Millipore). Tert-butyl alcohol (TBA; Merck, 99.5% pure) was used as received.

To ensure the absence of contamination, the surface tensions of all substances were measured prior to use, employing the Wilhelmy plate of a K10-ST tensiometer ($\pm 0.1 mN \cdot m^{-1}$). n-Heptane, TBA and water showed surface tensions of 20.5, 20.3 and 72.7mN·m⁻¹ at 293.15K, respectively. These tensions are in agreement with values reported by Jasper (1972) of 20.1, 20.0 and 72.9mN·m⁻¹, respectively.

The systems were prepared in vials with equal volumes of water and heptane. All reactants were weighted successively using an AB204 (Mettler Toledo) analytical balance (± 0.0001g). Different amounts of TBA were added to each vial in order to prepare thirty three mixtures with molar fractions of alcohol (x_{TBA}) between 0.0 and 0.1. Each flask was initially gently shaken and then left to equilibrate for a month to favor the partition of the alcohol between the organic and aqueous phase. Approximately 1.5ml of the aqueous phase of the vials was used to fill the capillary

of the tensiometer. Following, 20µl of the organic phase were added to the capillary using a syringe (SGE Company), and the interfacial tension of the system was measured using the spinning drop (see below). In order to determine the density of the liquid phases, three samples of 1ml were taken from each phase of the vial in order to evaluate their weight using an analytical balance.

Instrument

Interfacial tensions were measured using a TGG110-M3 spinning drop tensiometer made at the Universidad de Los Andes, Venezuela. The instrument consists of a glass capillary with an internal diameter 0.6mm, which is placed inside a rotating metal tube with two parallel rectangular windows (one on each side). From the back of the rotating tube, a stroboscopic lamp or a white light bulb is used to illuminate the oil drop. A DS150 OSX+PC camera placed on the opposite side of the capillary, allows taking pictures of the drop at different rotational velocities. These photographs are used later to determine the geometrical characteristics of the drop.

The method of Vonnegut (Vonnegut, 1942) consists in suspending a drop of phase 'A' in a capillary filled with an immiscible liquid 'B'. The capillary is subjected to a centrifugal force along its horizontal axis rotation, until the drop of the phase A adopts a cylindrical shape.

Following the centrifugal force is used to balance the surface tension. If the length of the cylindrical drop is considerably larger than its radius, the equation of Vonnegut can be applied (Vonnegut, 1942; Princen *et al.*, 1967):

$$\gamma = \Delta\rho\,\omega^2 R^3 \big/ 4 \qquad (1)$$

where γ: interfacial tension, $\Delta\rho$: difference in density between the immiscible phases, ω: angular velocity of the rotating tube, and R: radius of a cylindrical drop. Thus, a measurement of the radius of the drop when it adopts a cylindrical shape, allows determining the interfacial tension of the system.

Measurements

In order to change the temperature of the capillary, the rotating tube was surrounded by a double-walled metal cylinder whose temperature was regulated using a circulating bath (1160S from VWR). For each composition the variation of surface tension as a function of temperature was determined. At each temperature, the rotational speed of the instrument was increased until the longest axis of the drop (L) was at least 7 times longer than its width (R). A thirty minute period was awaited to attain a stable rotational speed. This was followed by an additional equilibration time of 3h at each temperature.

The tensions were obtained using Eq. 1. The measurement consisted in taking six photographs of the drop. The computer software allows evaluating the diameter of the cylindrical drop (±0.01mm) from the pictures. If the diameter of the drop is known along with the density difference between the phases, the interfacial tension can be calculated. The error bars of interfacial tension were obtained propagating the errors of $\Delta\rho$ and R in the formula.

The density difference between the phases ($\Delta\rho$) was calculated using the equilibrium gravimetric densities of the bulk phases of heptane and

water in the heptane/water/ TBA (H/W/TBA) system at T= 298K (Table I). In the most favorable case, this density difference has to be determined at each temperature for each alcohol concentration. Due to the lack of a density meter, the density of the phases at each composition was only evaluated at T= 298K. In order to estimate the possible influence of this limitation, approximate equations of the density previously employed in Vásquez *et al.* (2002) were used (see Eqs. 4 and 5 in Vásquez *et al.*, 2002). The partition constant of TBA was assumed to be equal to 1.0 with the sole purpose of this appraisal. Using the referred approximations, the predicted density difference ($\Delta\rho_p$) comes out to be systematically higher than the gravimetric determination at 298K ($\Delta\rho_m$). However, as will be shown below, the essential features of the curve of S^σ *vs* x_{TBA} do not change significantly due to this temperature dependence of $\Delta\rho$. This could possibly be due to the partial cancellation of errors when computing $\Delta\rho$, since the density of each liquid decreases as a function of the temperature.

The excess entropy S^σ was approximated by the variation

of the interfacial tension as a function of the absolute temperature (slope of γ *vs* T) at each alcohol concentration

$$S^\sigma = \partial\gamma/\partial T \qquad (2)$$

In this case the error bars resulted from a minimum-square fit of the data of γ *vs* T, taking into account the error in γ resulting from the propagation of errors of the Vonnegut formula.

Results

Using the present version of the spinning drop tensiometer, the interfacial tension of the clean H/W interface comes out to be 49.2 ±1.6mN·m⁻¹ at 298K. This value is close to the interfacial tension obtained by Zeppieri *et al.*, 2001 using pendant-drop technique 50.71 ±0.04mN·m⁻¹. However, the absolute magnitude of the error is larger.

Table II shows the data of tension and interfacial entropies obtained. The percentage dispersion with respect to the average interfacial tension $(\% D = 100\,\big|\gamma - \overline{\gamma}\big|\big/\overline{\gamma})$ is 3.5%. However, the absolute error of the entropy which results from the propagation of errors is significant, although it decreases considerably with the

increase of the alcohol concentration.

Figure 1 shows the typical result of a measurement of γ *vs* T at a constant alcohol concentration. The tension changes linearly as a function of the temperature, but the slope of the curve varies with the TBA concentration. Notice that the regression coefficients are very good. The worst regression coefficient of the set is 0.9990.

From the behavior of γ *vs* T at each concentration it is possible to reconstruct the variation of γ *vs* x_{TBA} for each temperature. Figure 2 shows the Gibbs adsorption isotherm for T= 298 K.

Despite the excellent linear regressions of γ *vs* T, the systems corresponding to TBA concentrations in the range $0.001 \le x_{TBA} \le 0.01$ show an appreciable dispersion of interfacial tensions with respect to the ideal form of the Gibbs adsorption isotherm. A similar behavior is observed at other temperatures. This might indicate that these concentrations of TBA require equilibration times longer than 3h in the capillary. In this regard it should be noticed that when a drop of oil is added to the capillary for the tension measurement, a fresh oil/water interface is

TABLE I
GRAVIMETRIC DENSITIES OF THE BULK PHASES OF HEPTANE AND WATER IN THE HEPTANE/WATER/TBA SYSTEM, AS A FUNCTION OF THE TBA CONCENTRATION (T= 298 K)

x_{TBA}	Aqueous phase $\rho \pm\Delta\rho$ (g·ml⁻¹)	Organic phase $\rho \pm\Delta\rho$ (g·ml⁻¹)	x_{TBA}	Aqueous phase $\rho \pm\Delta\rho$ (g·ml⁻¹)	Organic phase $\rho \pm\Delta\rho$ (g·ml⁻¹)
0	0.996 ±0.009	0.679 ±0.006	8.13×10⁻³	0.994 ±0.008	0.676 ±0.005
7.71×10⁻⁷	0.990 ±0.008	0.673 ±0.006	9.03×10⁻³	0.997 ±0.008	0.679 ±0.008
9.97×10⁻⁶	0.992 ±0.008	0.678 ±0.009	9.92×10⁻³	0.977 ±0.008	0.669 ±0.006
3.25×10⁻⁵	0.985 ±0.008	0.667 ±0.006	1.20×10⁻²	0.982 ±0.010	0.676 ±0.006
3.33×10⁻⁵	0.994 ±0.010	0.677 ±0.008	1.41×10⁻²	0.983 ±0.008	0.674 ±0.005
1.13×10⁻⁴	0.992 ±0.008	0.674 ±0.014	1.82×10⁻²	0.974 ±0.008	0.673 ±0.007
2.12×10⁻⁴	0.993 ±0.008	0.681 ±0.005	1.92×10⁻²	0.986 ±0.008	0.680 ±0.006
3.07×10⁻⁴	0.981 ±0.008	0.669 ±0.006	2.00×10⁻²	0.982 ±0.008	0.678 ±0.005
6.43×10⁻⁴	0.981 ±0.008	0.666 ±0.006	2.39×10⁻²	0.974 ±0.009	0.674 ±0.007
1.58×10⁻³	0.993 ±0.009	0.676 ±0.006	3.00×10⁻²	0.972 ±0.008	0.678 ±0.005
2.90×10⁻³	0.994 ±0.009	0.685 ±0.007	4.00×10⁻²	0.975 ±0.008	0.681 ±0.006
4.11×10⁻³	0.974 ±0.008	0.673 ±0.006	5.00×10⁻²	0.952 ±0.009	0.699 ±0.009
4.60×10⁻³	0.996 ±0.008	0.681 ±0.005	6.25×10⁻²	0.967 ±0.008	0.684 ±0.006
4.76×10⁻³	0.992 ±0.008	0.672 ±0.006	7.51×10⁻²	0.962 ±0.009	0.681 ±0.013
4.93×10⁻³	0.996 ±0.008	0.679 ±0.005	8.79×10⁻²	0.951 ±0.008	0.687 ±0.007
5.59×10⁻³	0.995 ±0.008	0.674 ±0.005	1.01×10⁻¹	0.960 ±0.008	0.705 ±0.007
7.10×10⁻³	0.996 ±0.008	0.677 ±0.005	———	———	———

TABLE II
INTERFACIAL TENSION (γ) AND INTERFACIAL ENTROPY (Sσ) OF THE HEPTANE/WATER SYSTEM AS A FUNCTION OF THE MOLAR FRACTION OF TERT-BUTYL ALCOHOL FOR SEVERAL TEMPERATURES.

x_{TBA}	γ (mN·m⁻¹)						$S^{\sigma} \times 10^{+3}$ (J·m⁻²·K⁻¹) †	r^2
	298K	303K	308K	313K	318K	323K		
0	49.2	48.8	48.5	48.1	47.8	47.4	0.069 ±0.077	1.0000
7.71×10^{-7}	45.0	44.7	44.3	44.0	43.7	43.4	0.066 ±0.067	0.9998
9.97×10^{-6}	44.2	43.9	43.6	43.2	42.9	42.6	0.064 ±0.065	0.9999
3.25×10^{-5}	43.5	43.2	42.8	42.5	42.2	41.9	0.064 ±0.065	0.9998
3.33×10^{-5}	42.6	42.3	42.0	41.7	41.4	41.0	0.063 ±0.076	0.9997
1.13×10^{-4}	39.3	39.0	38.7	38.4	38.1	37.8	0.059 ±0.089	0.9999
2.12×10^{-4}	38.9	38.7	38.4	38.1	37.8	37.5	0.058 ±0.059	0.9999
3.07×10^{-4}	35.5	35.0	34.4	33.9	33.4	32.9	0.103 ±0.052	0.9999
6.43×10^{-4}	33.8	33.3	32.8	32.3	31.8	31.3	0.103 ±0.049	0.9998
1.58×10^{-3}	37.4	36.9	36.3	35.8	35.2	34.7	0.110 ±0.058	0.9999
2.90×10^{-3}	28.3	27.9	27.5	27.0	26.6	26.2	0.083 ±0.044	0.9999
4.11×10^{-3}	31.7	31.2	30.7	30.3	29.8	29.3	0.094 ±0.047	0.9998
4.60×10^{-3}	34.7	34.2	33.7	33.2	32.7	32.3	0.097 ±0.051	0.9999
4.76×10^{-3}	36.5	35.7	34.9	34.1	33.4	32.6	0.152 ±0.052	0.9997
4.93×10^{-3}	31.7	30.7	29.8	28.9	28.0	27.2	0.182 ±0.046	0.9995
5.59×10^{-3}	31.6	30.6	29.7	28.8	27.9	27.1	0.180 ±0.044	0.9997
7.10×10^{-3}	26.6	25.7	25.0	24.0	23.0	22.3	0.173 ±0.038	0.9992
8.13×10^{-3}	28.5	27.6	26.8	26.0	25.2	24.4	0.163 ±0.040	0.9997
9.03×10^{-3}	34.9	33.9	33.0	32.0	31.1	30.2	0.188 ±0.049	0.9999
9.92×10^{-3}	27.5	26.3	25.1	24.0	22.8	21.7	0.230 ±0.039	0.9995
1.20×10^{-2}	24.5	23.4	22.3	21.2	20.2	19.2	0.212 ±0.041	0.9991
1.41×10^{-2}	22.5	21.4	20.4	19.5	18.5	17.6	0.194 ±0.031	0.9990
1.82×10^{-2}	18.6	17.7	16.9	16.1	15.3	14.5	0.165 ±0.028	0.9998
1.92×10^{-2}	18.0	17.4	16.8	16.1	15.4	14.8	0.130 ±0.027	0.9996
2.00×10^{-2}	18.0	17.4	16.8	16.3	15.8	15.3	0.108 ±0.027	0.9995
2.39×10^{-2}	15.2	14.8	14.3	13.9	13.4	13.0	0.088 ±0.024	0.9997
3.00×10^{-2}	12.5	12.1	11.8	11.4	11.0	10.6	0.075 ±0.019	0.9996
4.00×10^{-2}	9.6	9.1	8.7	8.3	7.9	7.5	0.081 ±0.014	0.9993
5.00×10^{-2}	6.6	6.2	5.9	5.5	5.1	4.7	0.078 ±0.011	0.9993
6.25×10^{-2}	5.4	5.1	4.7	4.4	4.0	3.7	0.066 ±0.007	0.9993
7.51×10^{-2}	4.8	4.6	4.4	4.2	4.0	3.8	0.040 ±0.011	0.9993
8.79×10^{-2}	3.9	3.7	3.5	3.3	3.1	2.9	0.041 ±0.006	0.9994
1.01×10^{-1}	3.1	2.9	2.7	2.5	2.3	2.1	0.037 ±0.005	0.9990

† The error was calculated using the propagation of errors of Eq. 1 and a linear regression of γ vs T.

Figure 1. Curves of interfacial tension γ (mN·m⁻¹) vs temperature (K) for a heptane/water system with: a: x_{TBA}= 0, b: x_{TBA}= 5.59×10^{-3} and c: x_{TBA}= 1.01×10^{-1}, where x_{TBA} is the molar fraction of tert-butyl alcohol (TBA).

created. Thus, the time required for the equilibration of this new interface is independent of the previous pre-equilibration time required for the appropriate partition of TBA between the immiscible phases of the vials. Despite these limitations, the linear dependence of the Gibbs isotherm is well characterized, and the overall qualitative shape of the curve is correct. Observe that the alternative procedure of building the isotherms at each temperature requires either a large number of capillaries to be equilibrated, or a large number of samples of each com-
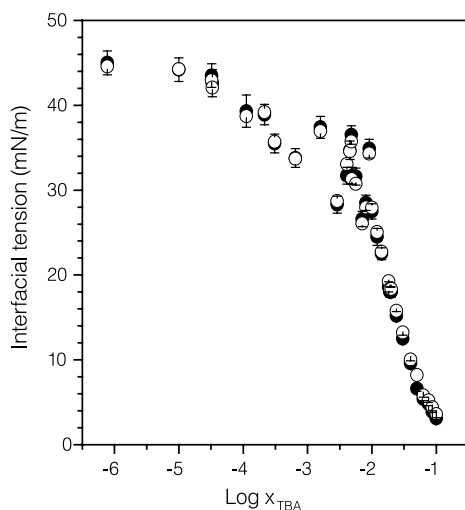

Figure 2. Gibbs adsorption isotherm of TBA at the heptane/water interface (T= 298K), using (●) the measured densities $\Delta\rho_m$ in g·ml⁻¹, or using (○) the estimated density difference $\Delta\rho_p$ in g·ml⁻¹ with Eqs. 4 and 5 from Vásquez et al. (2002).
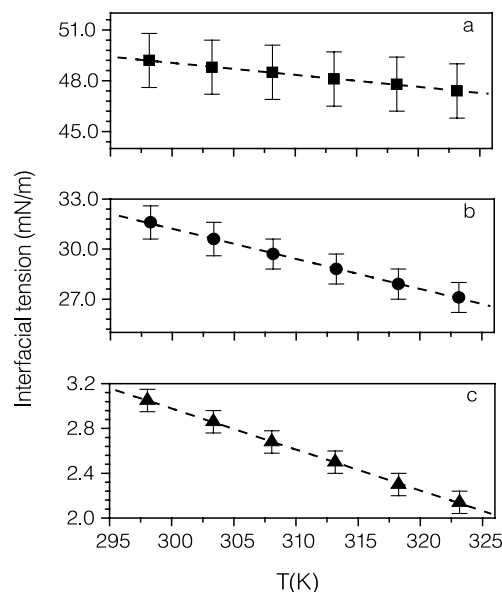
position. Notice also that for the experimental conditions employed, the values of $\Delta\rho$ do not affect significantly the shape of the adsorption isotherm.

Figure 3 shows the variation of interfacial entropy of the system composed by water (W), heptane (H) and TBA. Three maxima are clearly observed at x_{TBA}= 0.00158, S^{σ}= (0.11 ±0.06)×10⁻³J·m⁻²·K⁻¹ (at 'a' in Figure 3), x_{TBA}= 0.00559, S^{σ}= (0.18 ±0.04)×10⁻³J·m⁻²·K⁻¹ (at 'c'), and x_{TBA}= 0.00992 ~0.01, S^{σ}= (0.23 ±0.04) ×10⁻³J·m⁻²·K⁻¹¹ (at 'e'). Additionally, a broad maximum ('shoulder') appears to be present between x_{TBA}= 0.04 and 0.08. Notice that the principal maximum in this experiment is very well defined, and occurs at x_{TBA} ~0.01, S^{σ}= 0.23×10⁻³J·m⁻²·K⁻¹. The concentration and the value of the entropy are similar to the one found by Glinski et al. (1995) for aqueous solutions of TBA x_{TBA}= 0.01 (see Table II of Glinski et al., (1995), S^{σ}=

0.24×10⁻³J·m⁻²·K⁻¹). All referred peaks rise well above the base of the curve which occurs at the highest TBA concentration x_{TBA}= 0.10, S^{σ}= (0.037 ±0.005)×10⁻³J·m⁻²·K⁻¹.

In-between the maxima of surface entropy, four minima of interfacial entropy can be seen in Figure 3. They correspond to TBA concentrations of x_{TBA}= 0.0029, S^{σ}= (0.08 ±0.04)×10⁻³J·m⁻²·K⁻¹ (at 'b'), x_{TBA}= 0.00813, S^{σ}= (0.16 ±0.04)×10⁻³J·m⁻²·K⁻¹ (at 'd'), x_{TBA}= 0.03, S^{σ}= (0.08 ±0.02)×10⁻³J·m⁻²·K⁻¹ (at 'f'); and x_{TBA}= 0.0751, S^{σ}= (0.04 ±0.01)×10⁻³J·m⁻²·K⁻¹ (at 'g').

Figure 4 shows the values of the interfacial entropy calculated using the values of $\Delta\rho_p$ instead of $\Delta\rho_m$. The general form of the curve of S^{σ} vs x_{TBA} is preserved (see also Figure 3). However, quantitative differences appear. These are more pronounced below the principal maximum. In particular, the heights of the secondary peaks formerly located at x_{TBA}= 0.00158 and x_{TBA}= 0.00559 decrease considerably. In fact, the smallest secondary peak is now barely distinguishable.

The differences between Figures 3 and 4 demonstrate that the spinning drop technique is very sensitive to the density
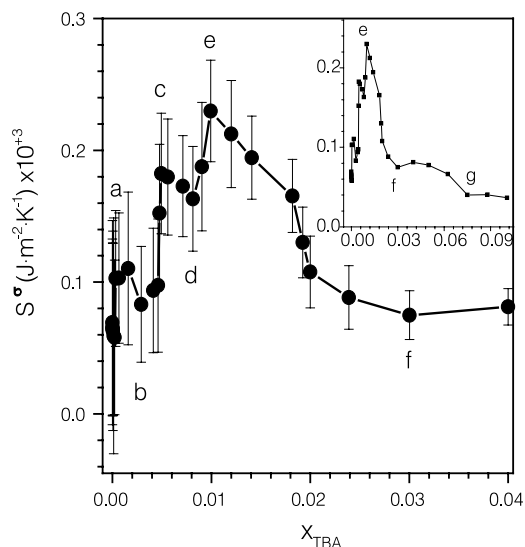
Figure 3. Excess interfacial entropy (S^σ) as a function of the molar fraction of TBA. The line drawn is only a guide to the eye. Three maxima at a: $x_{TBA}= 0.00158$, c: $x_{TBA}= 0.00559$, and e: $x_{TBA}= 0.00992$ are observed. The four observed minima occur at b: $x_{TBA}= 0.0029$, d: $x_{TBA}= 0.00813$, f: $x_{TBA}= 0.03$, and g: $x_{TBA}= 0.0751$.

Figure 4. Excess interfacial entropy (S^σ) as a function of the molar fraction of TBA, using estimated densities obtained from Eqs. 4 and 5 from Vásquez *et al.* (2002), as $\Delta\rho_m$ in g·ml⁻¹ (○). The lines drawn are only a guide to the eye. Error bars were not drawn in order to allow a clear observation of the secondary peaks.

difference between the immiscible phases. The number of critical points markedly depends on the exact value of $\Delta\rho$. In any event, the principal peak remains at the same position to the one previously found in Figure 3, and at least, one secondary maximum ('c') is clearly distinguishable.

Discussion

The spinning drop technique is known to be more reliable than the Wilhelmy plate and du Noüy ring methods for measuring interfacial tensions. The instrument employed uses the Vonnegut equation (Eq. 1) to calculate the tension. Consequently, the apparatus does not require the whole profile of the drop, but only its width. It was developed for low interfacial tensions where the deformation of the oil drop can be easily achieved at a moderate rotational speed. In fact, the error of the measurement ($\Delta\gamma$) depends on the value of the tension. The maximum error is 10% the value of the tension. Hence, the accuracy of the instrument increases with the decrease of the interfacial tension. This is well illustrated by the magnitude of the error bars in Figures 1a, b and c.

In order to check for the consistency of the data, the Gibbs adsorption isotherm was plotted for several temperatures. The one corresponding to T= 298K is shown in Figure 2. A large dispersion of the data is observed in the range $0.0001<x_{TBA}<0.01$. Such behavior suggests that despite the period of equilibration of one-month, the 0.5h waited for the stability of the rotational speed, and the 3h of additional equilibration of the liquids in the tensiometer, some of the systems appear to be out of equilibrium.

The magnitude of the error bars in Figure 3 does not allow establishing the existence of secondary critical points of interfacial entropy. Only the principal maximum at $x_f= 0.01$ survives the error analysis: the peak rises well above the base of the curve. Notice that some secondary maxima are defined by several experimental points. However, the absolute value of the excess entropy decreases when the density of the phases is extrapolated using approximate analytical equations (Figure 4).
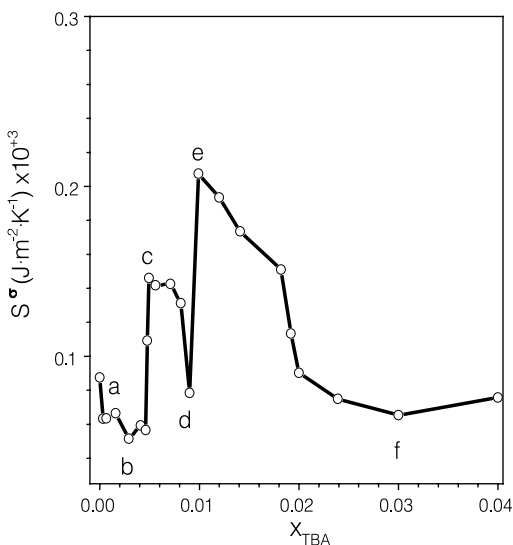
Moreover, some secondary signals (like point 'd' in Figure 4) change significantly. Hence, it could only be affirmed that a broad continuous distribution of interfacial entropy exists, with a maximum around $x_f= 0.01$.

Figure 5 shows a comparison of the present measurements with previous Wilhelmy-plate evaluations of the surface entropy corresponding to the water/TBA and heptane/TBA systems (Vásquez *et al.*, 2002).
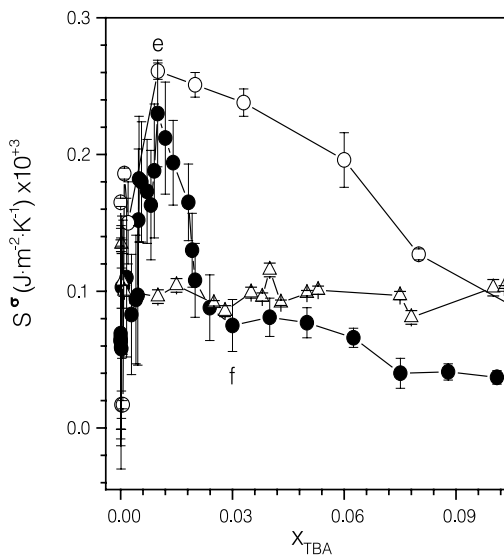

Figure 5. Excess interfacial/surface entropy (S^σ) as a function of the molar fraction of TBA for ●: heptane/water/TBA (present measurements), △: heptane/TBA and ○: water/TBA from Vásquez *et al.* (2002).

Since the Wilhelmy plate technique is only appropriate for the evaluation of the surface entropy, the fact that the H+TBA system does not show a pronounced maximum of entropy implies that water is required for this observation. These results strongly suggest that the principal peak of interfacial entropy observed in the systems made of W+TBA and W+H+TBA, have a common origin. Hence, the primary maximum might probably be caused by the presence of clathrate structures at the interface, as formerly proposed by Glinski *et al.* (1995).

In the previous evaluation of the interfacial entropy of the H/W/TBA system (Figure 6) using a Du Noüy ring (Vásquez *et al.*, 2002), only two maxima ($x_{TBA}= 0.00052$ and 0.00361) and two minima ($x_{TBA}= 0.00215$ and 0.0129) were clearly distinguished. Some of these signals could possibly be related to the set of critical points described above, but the highest value of S^σ previously found only reached 0.16×10^{-3}J·m⁻²·K⁻¹. This value is considerably lower than the ones reported in the present work. However, the present values are of a similar magnitude of the ones found by Glinski *et al.* (1995) for the aqueous solution of TBA. Moreover, the number of TBA concentrations studied in this report is considerably higher than before. As a result, the shape of the peaks is defined by more experimental points. Also, the difference between the highest and the minimum interfacial entropies observed in Figure 3 is considerably larger than the span of the critical points previously detected with the Wilhelmy plate (0.08×10^{-3}J·m⁻²·K⁻¹; Vásquez *et al.*, 2002). It is clear from Figure 6 that the Du Noüy ring produces very different results from the ones of the spinning drop tensiometer for the heptane/water/TBA system.

The existence of supra-molecular structures of mesoscopic scale was already found in numerical simulations of aqueous solutions of TBA (Finney et al., 2003). Furthermore, the appearance of a meso-heterogeneous phase in the same system has been recently detected by optical methods (Subramanian et al., 2011a). These findings could probably be related to the appearance of secondary maxima of the interfacial entropy in systems with TBA.

Recently, Subramanian and Anisimov (2011) and Subramanian et al. (2011) had convincingly demonstrated that in aqueous solutions TBA aggregation occur whenever propylene oxide (PPO) is present in the system. PPO is a surface-active by-product of the synthesis of TBA. Following this line of reasoning, it is possible that heptane could decompose during the long pre-equilibration period (one-month) giving rise to surface active peroxides and/or PPO. In this case, a maximum of entropy will be observed when a spinning drop tensiometer is used, but it will not be found with conventional tensiometers (with rings and plates), where the equilibration time only spans a few hours. This possibility can probably be ruled out in the future by repeating the experiments of plate and ring with a month-old sample of heptane, and/or analyzing the heptane phases employed in the experiments after the pre-equilibration period.

Conclusion

The interfacial entropy of a heptane/water interface shows a large maximum at $x_{TBA}= 0.01$. Based on the position of the principal maximum, its height ($S^\sigma= 0.23 \pm 0.04 \times 10^{-3} J \cdot m^{-2} \cdot K^{-1}$), the absence of a similar peak in a H/TBA system, and the presence of a large maximum in the W/TBA system at a similar concentration, it is concluded that the presence of wa-
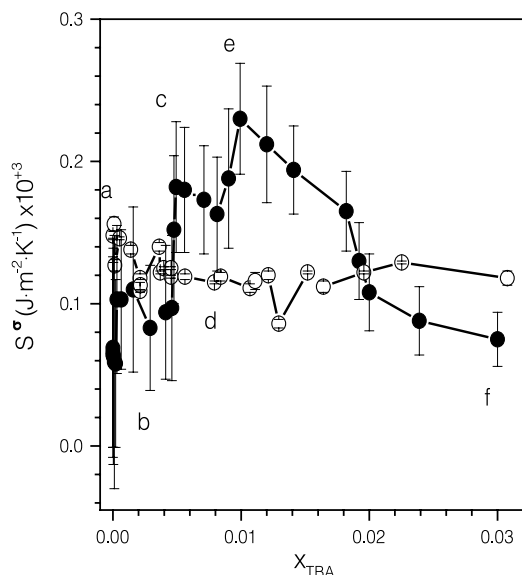

Figure 6. Excess interfacial entropy (S^σ) of the heptane/water/TBA system as a function of the molar fraction of TBA, obtained by means of ●: spinning drop tensiometer and o: du Noüy ring tensiometer.

ter is necessary for the observation of the phenomenon. This fact supports the former hypothesis (Glinski et al., 1995) regarding the existence of clathrates at the interface.

It is clear that despite its apparent simplicity, the process of evaluation of the interfacial entropy is laborious. This thermodynamic variable is very sensitive to changes in composition, temperature, and liquid density. However, the present results suggest that other secondary maxima of entropy could also exist (Vásquez et al., 2002) in the ternary system studied. Accurate density measurements at several compositions and temperatures are necessary in order to confirm the true existence of these signals.

REFERENCES

Aveyard R, Binks BP, Lawless TA, Mead J (1988) Nature of the oil-water interface and equilibrium surfactant aggregates in systems exhibiting low tensions. *Can. J. Chem. 66*: 3031-3037.

Bourrel M, Salager JL, Schechter RS, Wade WH (1980) A correlation for phase behavior of nonionic surfactants. *J. Colloid Interface Sci. 75*: 451-461.

Chavepeyer G, Gliński J, Platten JK (1995) Surface properties of dilute aqueous solutions of cyclohexyl and benzyl alcohols and amines. *New J. Chem. 19*: 1165-1170.

Finney JL, Bowron DT, Daniel RM, Timmins PA, Roberts MA (2003) Molecular and mesoscale structures in hydrophobically driven aqueous solutions. *Biophys. Chem. 105*: 391-409.

Glinski J, Chavepeyer G, Platten JK, De Saedeleer C (1993) Interfacial tension and interface phase transitions in two-phase water-long-chained alcohols systems. *J. Colloid Interface Sci. 158*: 382-387.

Glinski J, Chavepeyer G, Platten JK, Smet P (1995) Surface properties of diluted aqueous solutions of tert-butyl alcohol. *J. Chem. Phys. 102*: 2113-2117.

Glinski J, Chavepeyer G, Platten JK (1996) Surface properties of diluted aqueous solutions of normal propyl alcohol. *J. Chem. Phys. 104*: 8816-8820.

Glinski J, Chavepeyer G, Platten JK, Smet P (1998) Surface properties of diluted aqueous solutions of normal short-chained alcohols. *J. Chem. Phys. 109*: 5050-5053.

Glinski J, Chavepeyer G, Platten JK (1999) Untypical surface properties of aqueous solutions of 1,5-pentanediol. *Coll. Surf. A 162*: 233-238.

Graciaa A, Lachaise J, Cucuphat C, Bourrel M, Salager JL (1993) Improving solubilization in microemulsions with additives. 2. Long chain alcohols as lipophilic linkers. *Langmuir 9*: 3371-3374.

Healy RN, Reed RL, Carpenter CW (1975) A laboratory study of microemulsion flooding. *Soc. Pet. Eng. J. 259*: 78-100.

Iwasaki K, Fujiyama T (1977) Light-scattering study of clathrate hydrate formation in binary mixtures of tert-butyl alcohol and water. *J. Phys. Chem. 81*: 1908-1912.

Iwasaki K, Fujiyama T (1979) Light-scattering study of clathrate hydrate formation in binary mixtures of tert-butyl alcohol and water. 2. Temperature effect. *J. Phys. Chem. 83*: 463-468.

Jasper JJ (1972) the surface tension of pure liquid compounds *J. Phys. Chem. Ref. Data 1*: 841-984.

Johansson K (1974) On the importance of accurate surface temperature measurements when determining γ and dγ/dT for water as functions of T.*J. Colloid Interface Sci. 48*: 176-177.

Maestro A, Solé I, González C, Solans C, Gutiérrez JM (2008) Influence of the phase behavior on the properties of ionic nanoemulsions prepared by the phase inversion composition method. *J. Colloid Interface Sci. 327*: 433-439.

Princen HM, Zia IYZ, Mason SG (1967) Measurement of interfacial tension from the shape of a rotating drop. *J. Colloid Interface Sci. 23*: 99-107.

Romero CM, Jiménez E, Suárez F (2009) Effect of temperature on the behavior of surface properties of alcohols in aqueous solution. *J. Chem. Thermodyn. 41*: 513-516.

Salager JL, Morgan JC, Schechter RS, Wade WH, Vásquez E (1979) Optimum formulation of surfactant/water/oil systems for minimum interfacial tension or phase behavior *Soc. Pet. Eng. J. 19*: 107-115.

Subramanian D, Anisimov MA (2011) Resolving the mystery of aqueous solutions of ternary butyl alcohol. *J. Phys. Chem. B 115*: 9179-9183.

Subramanian D, Ivanov DA, Yudin IK, Anisimov MA, Sengers JV (2011) Mesoscale inhomogeneities in aqueous solutions of 3-methylpyridine and tertiary butyl alcohol. *J. Chem Eng. Data 56*: 1238-1248.

Urbina-Villalba G, Martín-Landrove R, Guaregua J (1997) Molecular dynamics simulation of the interfacial behavior of a heptane/water system in the presence of nonylphenol triethoxylated surfactants. 1. Surface energy, surface entropy, and interaction energies as a function of temperature and surfactant concentration. *Langmuir 13*: 1644-1652.

Vásquez D, Toro J, Lozsán A, García-Sucre M, Urbina-Villalba G (2002) Interfacial properties of tert-butyl alcohol solutions and their relation to clathrate formation *J. Phys. Chem. B. 106*: 2649-2655.

Vonnegut B (1942) Rotating bubble method for the determination of surface and interfacial tensions. *Rev. Sci. Instr. 13*: 6-9.

Zeppieri S, Rodríguez J, López-de-Ramos AL (2001) Interfacial tension of alkane + water systems. *J. Chem Eng. Data 46*: 1086-1088.